Title

The Transcription Factor ZNF217 Is a Prognostic Biomarker and Therapeutic Target during Breast Cancer Progression

Journal

Cancer Discovery, 2(7)

ISSN

2159-8274

Authors

Littlepage, Laurie E
Adler, Adam S
Kouros-Mehr, Hosein
et al.

Publication Date

2012-07-01

DOI

10.1158/2159-8290.cd-12-0093

Peer reviewed

The transcription factor ZNF217 is a prognostic biomarker and therapeutic target during breast cancer progression

Laurie E. Littlepage[1,2], Adam S. Adler[3,7], Hosein Kouros-Mehr[1,7], Guiqing Huang[1,2], Jonathan Chou[1,2], Sheryl R. Krig[4], Obi L. Griffith[5], James E. Korkola[5], Kun Qu[3], Devon A. Lawson[1,2], Qing Xue[1], Mark D. Sternlicht[1,2,8], Gerrit J. P. Dijkgraaf[1,7], Paul Yaswen[5], Hope S. Rugo[2], Colleen A. Sweeney[4], Colin C. Collins[2,9], Joe W. Gray[2,5,10], Howard Y. Chang[3,6], Zena Werb[1,2]

[1]Department of Anatomy, University of California, San Francisco, California 94143-0452
[2]Helen Diller Family Comprehensive Cancer Center, University of California, San Francisco, California 94143
[3]Program in Epithelial Biology, Stanford University School of Medicine, Stanford, California 94305
[4]Divison of Basic Sciences, University of California at Davis Cancer Center, Sacramento, California, 95817
[5]Life Sciences Division, Lawrence Berkeley National Laboratory, Berkeley, California 94720
[6]Howard Hughes Medical Institute

Present addresses:
[7]Genentech, South San Francisco, CA 94080
[8]FibroGen, 409 Illinois Street, San Francisco, CA 94158
[9]The Vancouver Prostate Centre, Vancouver, BC V5Z 1M9, Canada
[10]Department of Biomedical Engineering, Oregon Health & Science University, Portland, OR 97239

Corresponding Author:
Zena Werb, Ph.D.
E-mail: zena.werb@ucsf.edu; Phone: 415-476-4622; Fax: 415-476-4565

Running Title
ZNF217 overexpression promotes malignancy

Word Count: 5806 words

Keywords:
Breast cancer; metastasis; gene amplification; cancer stem cells; epithelial-mesenchymal transition; AKT; chemotherapy resistance

Abstract

The transcription factor ZNF217 is a candidate oncogene in the amplicon on chromosome 20q13 that occurs in 20-30% of primary human breast cancers and correlates with poor prognosis. We show that Znf217 overexpression drives aberrant differentiation and signaling events to promote increased self-renewal capacity, adult stem cell marker expression, mesenchymal marker expression, invasion and metastasis. By in silico screening, we identified candidate therapeutics that inhibit growth of cancer cells expressing high ZNF217 at low drug concentrations. We demonstrate that the nucleoside analog triciribine is an inhibitor of ZNF217 tumor growth and chemotherapy resistance, and inhibits signaling events (e.g., P-AKT, P-MAPK) in vivo. Our data suggest that ZNF217 is a biomarker of poor prognosis and a therapeutic target in breast cancer patients and that triciribine may be part of a personalized treatment strategy in patients overexpressing ZNF217. Since ZNF217 is amplified in numerous cancers, these results have implications for other cancers.

Significance

This study finds that ZNF217 is a poor prognostic indicator and therapeutic target in breast cancer patients and may be a strong biomarker of triciribine treatment efficacy in patients. Because previous clinical trials for triciribine did not include biomarkers of treatment efficacy, this study provides a rationale for revisiting triciribine in the clinical setting as a therapy for breast cancer patients who overexpress ZNF217.

Introduction

In the most aggressive breast tumors, neoplastic cells activate or amplify oncogenes, or inactivate or delete tumor suppressor genes to promote invasive growth and poor prognosis in patients. Amplification of the human chromosomal region 20q13 occurs in 20-30% of primary human breast cancers, as well as in other cancers, and its amplification correlates with poor patient prognosis (1, 2).

The ZNF217 gene on human 20q13.2 encodes a transcription factor that is overexpressed in all breast tumors and cell lines in which the gene is amplified, as compared to normal mammary tissue and epithelial cells (1, 2). The ZNF217 protein is a member of the C_2H_2 family of transcription factors and contains eight predicted Kruppel-like C_2H_2 zinc finger motifs and a proline-rich region. It is a component of a human histone deacetylase complex (CoREST-HDAC) and is found in complexes with the transcriptional co-repressor C-terminal binding protein (CtBP), the histone demethylases LSD1 (H3K4, H3K9) and KDM5B/JARID1B/PLU-1 (H3K4), and the methyltransferases G9a (H3K9, H3K27) and EZH2 (H3K27) (3-8). Its overexpression in human mammary epithelial cells (MECs) overcomes senescence and promotes immortalization accompanied by increased telomerase activity, increased resistance to TGFß-induced growth inhibition, and amplification of c-Myc (9). ZNF217 binds to the promoters of genes involved in differentiation and is repressed following retinoic acid treatment of pluripotent embryonal cells (10).

Recently a connection has emerged between the undifferentiated, stem cell-like phenotype in breast cancer cells and transdifferentiation of the tumor

cells towards a mesenchymal phenotype [reviewed in (11-13)]. Induction of epithelial-to-mesenchymal transition (EMT) in cultured MECs not only increases the population of cells with mesenchymal markers but also increases those with progenitor cell characteristics ($CD44^{high}/CD24^{low}$) (14). During tumor progression, EMT and the expanded progenitor population together may contribute to cell plasticity.

In this study we have investigated whether and how Znf217 promotes tumor progression and poor prognosis. We used cultured cells, in vivo transplant models and human patient expression datasets, to determine whether Znf217 promotes an accelerated tumor progression phenotype, and is therapeutic target.

Results

ZNF217 is Prognostic of Poor Survival in Breast Cancer Patients

Using microarray expression data from primary breast tumors and corresponding clinical data (15, 16), we found that high ZNF217 amplification and expression correlate with shorter overall survival, reduced disease-specific survival, and relapse-free survival (Figures 1A-B, S1A-B). In a meta-analysis of relapse-free survival across nine published studies that included 858 patients (ER+HER2-LN-) with ZNF217 expression, we found that ZNF217 expression was significantly associated with 5 yr (P=0.012) and 10 yr (P=0.023) relapse status (Mann-Whitney), and that patients with relapse had higher ZNF217 expression. Similarly, patients grouped into the high expression tertile had significantly worse

survival than low expression groups (Figure 1C). These data show that ZNF217 is prognostic of poor survival in patients by univariate analysis. Moreover, ZNF217 was a better predictor of survival than ER status by multivariate analysis (Figure S1C).

Overexpression of Znf217 Accelerates Loss of Adhesion and Increased Motility in Mouse Mammary Epithelial Cells

To determine the consequences of Znf217 overexpression, we generated mouse mammary epithelial cell lines that overexpressed Znf217 by retroviral and lentiviral infection. Mouse mammary epithelial cell lines (SCp2, NMuMG, EpH4) overexpressing Znf217 had altered motility showing a more scattered phenotype than adherent, clustered control cells (Figures 2A-C, S2A-C). In a wound healing/scratch assay, SCp2 cells (Figure 2D) and NMuMG cells (data not shown) overexpressing Znf217 showed increased motility as individual cells, extended lamellipodia forward and migrated separately from other cells to the middle of the scratch (Figure 2D and Movie S1). In contrast, vector-treated cells migrated as a sheet predominantly with a single leading edge. In keeping with the increased motility, cells overexpressing Znf217 reorganized their actin cytoskeleton with reduced cortical actin and increased actin stress fibers (Figure 2E) and upregulated EMT markers including Snail1 and Twist (Figure 2F). Consistent with these results, we found ZNF217 expression levels correlated with expression of EMT markers including Snail1, Snail2 and Vimentin, genes that have ZNF217 enriched at their promoters in human breast cancer cell lines and

tumors (Table S1). Taken together, these results indicate that the early effects of increased ZNF217 expression would lead to premalignant changes of enhanced mammary epithelial growth and migration.

We used gene expression microarrays of the mouse SCp2 MECs overexpressing Znf217 to identify altered processes and molecular targets of Znf217 (Figure 2G). In these cells, 176 genes were upregulated and 243 genes downregulated following Znf217 overexpression. We used DAVID software to classify the gene sets with gene ontology (GO) terms (Table S2). The GO terms suggested that Znf217 overexpression promoted increased cell motility, decreased epithelial differentiation, increased vasculature development and changes at the membrane.

We also assayed for clonogenicity and transformation potential in vitro. Znf217 overexpression in NIH3T3 cells stimulated anchorage independent growth in a soft agar assay, with increased number and size of colonies (Figure 3A-C).

Znf217 Overexpression in Normal Primary Mammary Epithelium Promotes Increased Mammosphere Formation in Culture

Because we found that Znf217 overexpression in culture promoted increased motility, decreased epithelial marker expression/increased mesenchymal marker expression and increased clonogenicity/transformation potential in vitro, we reasoned that these changes were consistent with a change in differentiation towards a less differentiated or more mesenchymal phenotype. Znf217 gene

expression was enriched in $CD24^{Med}CD49f^{High}$ cell population, which includes basal, myoepithelial and progenitor cells, compared to $CD24^{High}CD49f^{Low}$ cells, which include luminal and luminal progenitor cells (Figure 3D-E).

To determine if Znf217 could promote an increase in a population of cells with progenitor cell phenotypes, we overexpressed Znf217 in normal primary MECs and analyzed the epithelial differentiation state and clonogenicity potential in the mammosphere assay. Primary MECs infected with a Znf217-overexpressing lentivirus overnight and then grown in serum-free nonadherent culture conditions demonstrated increased self-renewal capacity as assessed by the mammosphere assay (Figure 3F-G).

Gene Expression Analysis of Mammary Epithelial Cells Following Znf217 Overexpression Predicts Changes in Epithelial Proliferation, Cell Adhesion and Motility

We next determined the impact of Znf217 overexpression on global gene expression in normal primary mouse MECs by gene expression microarrays (Figure 3H). Primary MECs were infected with a Znf217-overexpressing lentivirus, passaged to expand the population, and confirmed to overexpress Znf217 by reverse transcription quantitative PCR (rt-qPCR) (Figure 3I). In these MECs, 340 genes were upregulated and 401 genes downregulated following Znf217 overexpression (Figure 3H). The GO terms classified by DAVID software (Table S2) suggest that Znf217 overexpression altered the gene expression profile of genes involved in cell proliferation, cell adhesion, cell migration, G-

protein coupled receptor signaling pathways and ribosomal function.

Genes identified by microarray analysis suggested that overexpressing Znf217 in vivo would promote increased epithelial growth or progenitor cell expansion (Figure 3H, Table S2). These genes included a number of TGFß and Wnt pathway genes (Axud1/Csrnp-1, Bcl9l, Bmper, Bmpr2, follistatin, Samd9l, Sfrp1, Tcf4, Tgfß2, Tgfßr3, Wnt5a). We validated selected genes including Wnt5a and Sfrp1 by rt-qPCR (Figure 3J). These results are consistent with Znf217 promoting differentiation towards a less differentiated cell-like phenotype via aberrant signaling in the TGFß and Wnt pathways.

We also examined epithelial marker expression in our microarray dataset. We found increased expression of both K17 (myoepithelial marker) and K18 (luminal epithelial marker) expression (Figure 3H). Consistent with these results, we found ZNF217 expression levels correlated with expression of K19 and K8/18, genes that have ZNF217 enriched at their promoters in human breast cancer cell lines, tumors and after knockdown in MCF7 cells (Tables S1, S3).

Znf217 Overexpression in Primary Mammary Epithelial Cells Drives an Adult Stem Cell Expression Signature

Because the aberrant differentiation markers seen both in vivo and in culture suggest that Znf217 may push mammary epithelial cells to a more progenitor cell-like phenotype, we compared our microarray dataset with our previously published stem cell signature of adult stem cells, which is downregulated in many epithelial cancers relative to normal tissue (17). Primary MECs overexpressing

Znf217 significantly repressed genes of the adult stem cell signature (Table S4; P=1.89x10^{-10}). Consistent with the increased clonogenicity by mammosphere assay, this overlap in expression signature suggests that Znf217 might block differentiation or promote self-renewal.

Tumors Overexpressing Znf217 Have a More Basal Pathology with Increased Dual Positive Luminal and Basal Cell Marker Expression

Our finding that Znf217 overexpression promoted changes in differentiation in normal and immortalized mammary epithelium prompted us to determine if these changes also followed in tumorigenic mammary epithelium both in culture and in vivo. We overexpressed Znf217 by lentiviral delivery of Znf217 into primary luminal-type mammary epithelial tumor cells isolated from 18-week-old MMTV-PyMT mice (PyMT MEC) or a MMTV-PyMT cell line (Vo-PyMT), sorted the cells for the IRES-Tomato reporter gene, and confirmed Znf217 overexpression by rt-qPCR (Figure 4A). In culture, Znf217 induced mesenchymal marker expression, reduced expression of E-cadherin and increased expression of EMT markers Snail2 and Twist (Figure 4A) and produced a more scattered phenotype (Figure S2C). In addition, cells overexpressing Znf217 readily formed increased numbers of mammospheres compared to the vector control cells (Figure 4B-C).

When the sorted cells were transplanted into syngeneic mouse mammary fat pads cleared of epithelium Znf217 overexpression accelerated the rate of tumor formation, reduced the tumor-free survival and increased both tumor volume and final tumor weight (Figures 4D-F, S3A). Tumors overexpressing

Znf217 had a markedly altered, heterogeneous histology compared to tumors from vector-treated cells (Figure 4G). Control tumors had little to no SMA staining with predominantly luminal $K8^+$ epithelium, while the Znf217 overexpressing tumors expressed higher levels of myoepithelial and myofibroblast SMA protein (Figure 4H).

Tumor cells from vector-treated cohorts were predominantly K8+, with few K14+ cells; most of the K14+ cells were K8- and were located basal to the K8+ tumor cells. Znf217 overexpression increased numbers of K14+ cells in tumors, with many double-positive K8+K14+ cells (Figures 4I-J and data not shown). The K8+K14+ cells may be a bipotent progenitor population capable of forming both luminal and myoepithelial cells, also seen by others as K18+K19+ cells (18-22).

We also assayed for epithelial E-cadherin expression in these tumors. In vivo Znf217 overexpression resulted in heterogeneous staining of E-cadherin with a large number of regions containing a marked reduction in E-cadherin expression, whereas control tumors had E-cadherin localized to the plasma membrane and present throughout the epithelium (Figures 5A, S3B).

Taken together, these phenotypic changes seen within the tumors are consistent with Znf217 promoting the acquisition of a mesenchymal/progenitor cell phenotype.

Overexpression of Znf217 Promotes Metastasis

Since metastasis in vivo often is accompanied by increased motility, invasive, and mesenchymal/basal phenotypes, we next asked if Znf217 promotes

metastasis in vivo. In mice transplanted with either PyMT or Vo-PyMT cells, Znf217 overexpression significantly increased the percentage of mice with lung metastases, increased metastatic burden and increased the number of spontaneous lung metastases per mouse (Figures 5B-D, S3C). In keeping with these results, high ZNF217 expression was prognostic of reduced metastasis-free survival in breast cancer patients (Figure 5E) (23).

ZNF217 Promotes Resistance to Chemotherapy

Patients with tumors expressing stem cell-like/progenitor cell markers have increased resistance to chemotherapy (24). Using clinical data in conjunction with expression data from patients who had received neoadjuvant chemotherapy with either doxorubicin or a combination of 5-fluorouracil and mitomycin (FUMI) before surgical removal of the tissue (16), we observed that patients with high ZNF217 expression were significantly less responsive to chemotherapy than were low ZNF217 patients (Figure 6A). High ZNF217 was also predictive of a reduced pathological complete response in patients who received chemotherapy only after surgical removal of the tumor (25) (Figure 6A).

ZNF217 Levels are Related to Levels of Activated AKT, MAPK and ERBB3

ERBB3 is a direct target of ZNF217 (26). To determine the mechanism underlying the effects of ZNF217, we analyzed several downstream signaling molecules downstream of ERBB3 in two human breast cancer cell lines (MCF7, ZR-75-1) that express high levels of ZNF217. We used both wild type cells and

cells after knock down for ZNF217 expression by siRNA, as described previously (26). We treated cells that were serum-starved overnight with the growth factor ligand for ERBB3, heregulin/neuregulin (HRG). Cells containing ZNF217-siRNAs consistently required higher concentrations of heregulin to induce ERBB3 signaling, phospho-AKT and phospho-MAPK (Figures 6B-C and S4A-D). These data indicate that these pathways are downstream of ZNF217 and that ZNF217 sensitizes cells to heregulin.

ZNF217 is a Drug Target for Individualized Therapy

Since ZNF217 is overexpressed in poor prognostic and chemoresistant breast cancer patients, we sought to identify drugs that kill tumor cells that overexpress ZNF217. We first used a candidate approach to determine if AKT pathway inhibitors promoted cell death in a ZNF217-dependent manner, since ZNF217 is required for and promotes AKT activation [Figure 6B-C and (27)]. MCF7 cells were infected with virus expressing shRNAs to ZNF217 and validated for reduced protein expression (Figure S4E-F). Assaying cell death of MCF7 cells infected with lentivirus expressing scrambled or ZNF217 shRNA knockdown constructs, we observed that the PI3K inhibitor GDC0941 and the AKT inhibitor MK2206 did not induce ZNF217-dependent cell death (Figure 6D).

We next used an in silico screening approach to identify candidate therapeutics that inhibit growth of cancer cells expressing high ZNF217 at low drug concentrations. We determined ZNF217 expression by rt-qPCR in the NCI60 panel of cell lines. We then used a drug dataset from a panel of ~50,000

drugs generated by the NCI Developmental Therapeutics Program (dtp.nci.nih.gov). Correlation of ZNF217 expression in the cell line panel with the drug panel identified 15 drugs that selectively inhibited growth of cells expressing high levels of ZNF217, as assessed by GI50, with a low drug concentration (Table S5).

To determine if ZNF217 contributes to the drug-induced growth inhibition, we assayed cell death of MCF7 cells infected with lentivirus expressing stably integrated scrambled or ZNF217 shRNA knockdown constructs. As proof-of-concept, we tested bisacodyl, triciribine, nogalamycin and 2E3E for their ability to influence cell death in culture in a ZNF217-dependent manner. Cells expressing reduced levels of ZNF217 (shRNA-ZNF217) required higher concentrations of bisacodyl or triciribine for cell killing (Figure 6E-F). Three different ZNF217-shRNA constructs gave similar results (Figure 6 and data not shown). Nogalamycin or 2E2E treatment did not promote ZNF217-dependent cell death at a therapeutically possible concentration range (data not shown).

We focused on triciribine (also known as API-2), which is a nucleoside analog and DNA synthesis inhibitor that has been tested in Phase I clinical trials in cancer patients as well as in one Phase II clinical trial in metastatic breast cancer patients (28-31). Cancer cells expressing high levels of ZNF217 required lower concentrations of triciribine to inhibit growth than cells with low ZNF217 expression (Figure 6G-H). We then assayed triciribine on a panel of breast cancer cell lines that we previously analyzed for gene expression (32). The GI50s were significantly correlated with ZNF217 expression levels (r=-0.39,

P=0.035 Spearman) (Figure 6I), consistent with a selective effect of triciribine on cell lines that express the highest ZNF217 levels.

Triciribine Kills Cells that Overexpress Znf217 in vivo

To test the effects of triciribine in vivo, we transplanted vector control and Znf217-overexpressing tumorigenic Vo-PyMT cells orthotopically to contralateral mammary fat pads cleared of epithelium. At three weeks, we injected mice with either triciribine or vehicle solution for five days per week. Triciribine treatment significantly reduced to baseline levels the increase in tumor burden seen as a result of Znf217 overexpression, and led to reduced phospho-AKT expression, reduced phospho-MAPK expression and increased cell death in vivo (Figures 7A-B, S7G). In culture, triciribine inhibited only phospho-AKT and did not inhibit phospho-MAPK or ErbB3 activation after heregulin stimulation (Figure 7C). The observed differences between signaling events inhibited by triciribine in culture versus in vivo suggest that cells within a tumor microenvironment respond differently to triciribine than do cells in culture.

Triciribine also was effective in vivo at inhibiting tumor growth in mice xenografted with the human tumorigenic cell line MCF7 compared to control treated mice (Figure 7D).

Triciribine Overcomes ZNF217-induced Doxorubicin Resistance

Tumor cells overexpressing ZNF217 are resistant to doxorubicin-induced cell death (27). Several groups have found triciribine to be an effective, synergistic

therapy in combination with other drugs (e.g., trastuzumab, farnesyltransferase inhibitors) to reduce tumor burden (33, 34). Similarly, we found that the addition of triciribine with doxorubicin to cells in culture generated a synthetic lethality in which cells overexpressing ZNF217 were no longer resistant to doxorubicin and instead were killed (Figure 7F). Interestingly, the parent mammary epithelial cell line HBL100 expresses low levels of adenosine kinase, which is required for the phosphorylation and activation of triciribine in patients. This suggests that ZNF217 may be a sufficiently predictive biomarker of triciribine efficacy, even in patients with low adenosine kinase, if patients are also treated in combination with a drug such as doxorubicin.

Discussion

ZNF217 is a Biomarker of Disease Progression and Treatment Response and is a Therapeutic Target Inhibited by Triciribine

In this study we identified ZNF217 as a prognostic biomarker of reduced survival, metastasis and chemoresistance in breast cancer patients. Using both cultured cells and in vivo mouse transplant models, we found that ZNF217 overexpression contributes to multiple aspects of carcinogenesis including increased proliferation/decreased cell death, increased invasiveness, increased motility, immortalization, chemotherapy resistance, metastasis and progenitor cell expansion. Our data demonstrate that Znf217 promotes carcinogenesis by driving a differentiation gene expression signature towards a less differentiated/progenitor state indicative of expanding a multipotent progenitor population.

We identified a panel of drugs that inhibit the growth of cell lines that overexpress ZNF217 and validated two that induced ZNF217-dependent cell death.

Triciribine: a Component of Therapy for Poor Prognostic Breast Cancer Patients

Triciribine is a nucleoside analog and DNA synthesis inhibitor that has been tested in Phase I clinical trials in cancer patients as well as in one Phase II clinical trial in metastatic breast cancer patients (28-31). In the Phase II study,

one of 14 patients had stable disease and the other patients progressed (31). The Phase II studies and subsequent studies found that triciribine was not readily bioactive in all patients, possibly due to the requirement for expression of multiple genes for triciribine bioactivation. Later studies identified triciribine as an allosteric inhibitor of AKT activation: it physically interacts with AKT to prevent AKT recruitment to the plasma membrane and to block the phosphorylation and activation of AKT (35, 36).

While several studies identified triciribine as an AKT inhibitor, triciribine is not always redundant with other AKT pathway inhibitors in treating tumors: often triciribine is more effective in vivo than other PI3K/AKT pathway inhibitors at inhibiting tumor progression (33). In contrast to triciribine treatment of cell lines in culture, we found that triciribine inhibited not only AKT activation but also MAPK activation in vivo (Figures 7B-C, 7E). We hypothesize that triciribine inhibits both AKT and MAPK pathways, both of which are downstream of ErbB3/ErbB2 activation. This could provide a rationale for inhibition of ZNF217-induced tumor burden by triciribine, since ZNF217 drives the overexpression of ErbB3 and leads to the activation of both AKT and MAPK pathways. Alternatively, triciribine could inhibit these pathways after activation of other receptor tyrosine kinases (RTKs) (Figure 7G).

Our study suggests that ZNF217 may be a sufficiently predictive biomarker of triciribine efficacy if patients are also treated in combination with a drug such as doxorubicin or another drug that offers synergy with triciribine (33) (34). In part, ZNF217 may act by inducing upregulation of its target ERBB3 (26).

Thus, cells resistant to triciribine treatment might independently activate multiple signaling pathways, making them less responsive to inhibitors that act upstream in the signaling pathway.

Combinatorial pathway activation may be therapeutically important in treating patients with high ZNF217 expression, as concurrent activation of the PI3K/AKT and RAS/MAPK pathways causes resistance to AKT inhibition in cells (37). Interestingly, in the panel of immortal cell lines expressing ZNF217 and tested for triciribine sensitivity, all outlier cell lines (i.e., lines with high GI50s and high ZNF217 expression) contained previously identified mutations in the PI3K/AKT and/or RAS/MAPK pathways (38-40). Since triciribine does not inhibit upstream activators PI3K or PDK1 or related family members directly (35), future studies will be required to sort out mechanistically how ZNF217 activates and triciribine inhibits signaling. Whether combination therapies will be more effective in vivo remains to be tested.

ZNF217 Reprograms Tumor Cells to Express Luminal and Myoepithelial Cell Markers

We found that Znf217 promotes phenotypes suggestive of expansion of progenitor cells in vivo and in culture and drives downregulation of an adult stem cell gene expression signature that is also downregulated in many epithelial cancers. Consistent with a progenitor phenotype, ZNF217 promotes increased telomerase, resistance to TGFß growth inhibition, and amplified c-MYC (9, 41), as well as chemotherapy resistance (27). That Znf217 may drive a less

differentiated gene expression signature is supported by the observation that Znf217 is upregulated in the somite following the transition from the presomitic mesoderm and prior to the differentiation into the skeleton, muscle and dermis (42). Moreover, Znf217 is repressed concurrently with Oct4 following differentiation of a teratocarcinoma cell line to neuronal cells and binds to the promoters of a number of genes involved in differentiation (10). Thus, in tumors ZNF217 may promote the transdifferentiation to or expansion of a pool of progenitor-like cells by aberrantly suppressing differentiation pathways.

Znf217 reprogrammed tumor cells to express both luminal and myoepithelial cell markers. Znf217 overexpression in tumor cells derived from mice expressing the oncogene PyMT switched their phenotype from a predominantly luminal to a more heterogeneous pathology characterized by expression of both luminal and myoepithelial epithelial cell markers. This phenotype is similar to that seen following Wnt1 overexpression or activation of the AKT pathway by PTEN deletion in vivo (43, 44). Interestingly, the PyMT oncogene can give rise to tumors expressing both luminal and myoepithelial markers, depending on the cell type into which it is introduced. Expression of PyMT by intraductal injection of avian retrovirus (RCAS-PyMT) induces tumors with a more rapid tumorigenesis and greater heterogeneity than seen in MMTV-PyMT mice (45). These tumors express markers of luminal, myoepithelial and progenitor cells. Likely the cell of origin is an immature or progenitor cell population.

Conclusion

We used an integrated biological approach to model the multiple contributions of ZNF217 to carcinogenesis during tumor progression, metastasis and during neoadjuvant treatment. We propose that ZNF217 is a biomarker that is prognostic of disease progression and is a therapeutic target. Our data suggest that triciribine may be a component of an effective treatment strategy in patients who have tumors expressing high ZNF217, possibly by targeting a progenitor population and reducing signaling in the AKT and MAPK pathways. Since ZNF217 is amplified in numerous cancers, this work has implications for other cancers as well.

Materials and Methods

Additional descriptions of materials and methods, including cell lines, antibodies, and staining procedures used, are in the Supplemental Data.

Mouse Lines Used in This Study

All mice used in this study were maintained on the FVB/n background and maintained under pathogen-free conditions in the UCSF barrier facility. Our animal protocols were reviewed and approved by the UCSF Institution Animal Care and Use Committee.

Metastasis analysis

Both PyMT MEC and Vo-PyMT transplants were analyzed for lung metastasis. To determine metastasis frequency, lung tissue blocks were sectioned into 5-mm sections and stained by hematoxylin and eosin (H&E). For each mouse analyzed, one section was scored for number of metastases seen at 100x magnification in 3 (PyMT MECs) or 5 (Vo-PyMT cell line) high-powered fields in regions of the tissue section with the highest density of metastases. Each cohort had 6-11 mice analyzed.

Statistical analysis

Statistical analysis was performed using Prism 4 software (GraphPad Software,

Inc.) or SPSS Statistics software (IBM) for Cox proportional hazard tests (Figure S1). Cohorts of three or more samples were compared using one-way analysis of variance (ANOVA). All tests used and *P* values are specified in the figure legends. $P<0.05$ was considered significant.

Supplemental Data

Supplemental Data include Supplemental Materials and Methods, 4 Supplemental Figures, one movie and 5 Supplemental Tables.

Accession Numbers

Microarray data were deposited to the NCBI's GEO Repository and are accessible to reviewers through GEO series accession number GSE24727.

Acknowledgments

The authors thank members of the Werb laboratory for helpful discussions throughout this project. We also thank Ying Yu for genotyping, Elena Atamaniuc for tumor measurements and Jimmy Hwang for statistical advice. The authors disclose no conflicts of interest.

Grant Support

This work was supported by grants from the National Institutes of Health (CA129523 and CA129523-02S1 to Z.W., CA058207 to J.W.G. and Z.W., and

ES012801 to Z.W. and P.Y.), a Stand Up to Cancer-American Association for Cancer Research Dream Team Translational Cancer Research Grant SU2C-AACR-DT0409 (to Z.W. and J.W.G.), an American Cancer Society Postdoctoral fellowship and a Ruth L. Kirschstein National Research Service Award CA103534 (to L.E.L.), a Canadian Institutes of Health Research Postdoctoral fellowship (to O.L.G.) and a Career Development Award from Bay Area Breast Specialized Programs of Research Excellence CA058207 (to M.D.S.).

Figure Legends

Figure 1. ZNF217 overexpression is a prognostic indicator in breast cancer patients.(A) Patients (n=118) were separated into high (n=59) vs. low (n=59) ZNF217 expression and analyzed for overall survival (*P*=0.003; Logrank). (B) Relapse-free survival based on high (n=40) vs. low (n=41) ZNF217 expression (*P*=0.01; Logrank). (C) Patients (n=858) were separated into low (n=286), intermediate (n=286), and high (n=286) ZNF217 expression and analyzed for relapse-free survival. Patients with high ZNF217 expression had worse survival than low ZNF217 patients (*P*=0.03; Logrank).

Figure 2. Znf217 overexpression promotes increased cell motility and a change in epithelial marker expression. (A) Relative expression of Znf217 expression levels by rt-qPCR in SCp2 mammary epithelial cell lines infected with virus to overexpress vector or Znf217. Results are comparable to results seen in three experiments. Each sample was tested by qPCR in triplicate relative to the reference TBP, with similar results for other reference genes. Graphs show the mean ± S.E.M. (B) Western blot analysis of Znf217 protein levels (anti-Znf217) and a loading control (anti-HDAC1). These images are representative of multiple experiments using retrovirus or lentivirus overexpression of Znf217. Arrows mark the indicated proteins. (C) Brightfield images of SCp2 mammary epithelial cells ± Znf217 display increased cell scattering in culture after Znf217 overexpression. (D) Frames from movies of SCp2 cells infected with vector or Znf217 following a scratch with a pipette tip. The movies ran 20.25 hours. Note the lamellipodia (arrow) extending from the cells by 5.5 hours and the increased number of Znf217-expressing cells in the middle of the scratch by 10.5 hours (arrow). (E) Phalloidin staining of SCp2 cells ± Znf217. (F) Relative expression of Znf217 and selected genes by rt-qPCR from NMuMG (top) and SCp2 (bottom) cells overexpressing vector or Znf217 in vitro. Graph shows the mean ± S.E.M., relative to the reference GAPDH. Similar results were seen with the reference HPRT. For each gene, samples for Znf217 were compared to vector by Mann-

Whitney tests, and significant *P* values <0.02 were marked with *. (G) Heat map of selected genes enriched following Znf217 overexpression in SCp2 MECs.

Figure 3. Znf217 overexpression causes an increase in soft agar colonies and in mammosphere formation. (A) Western blot analysis of Znf217 overexpression in NIH3T3 cells infected with vector or Znf217 retrovirus. (B) Znf217 overexpression increases the number of colonies by anchorage-independent growth in soft agar assay. Relative number of colonies per well by soft agar for vector or Znf217 overexpressing cells (*P*=0.001; Student's t test). Graph compiles results from three experiments, each done in triplicate. (C) Znf217 overexpression increases the size and number of colonies in soft agar assay. Brightfield images of anchorage-independent colonies from soft agar assay. Arrows mark examples of colonies. The large colonies were only seen for the Znf217 overexpressing cells, while much smaller colonies seen for the vector expressing cells. (D) Relative expression of Znf217 by rt-qPCR from normal adult mammary gland (FVB/n), relative to the reference HPRT with line marking the mean. Glands were sorted by flow cytometry for $CD24^{Med}CD49f^{High}$ (basal/myoepithelial/progenitor cells) and $CD24^{High}CD49f^{Low}$ (luminal/luminal progenitor) fractions, and RNA was isolated and used to generate cDNA from each population. Each dot represents one mouse sorted, collected and processed by rt-qPCR. Graph shows relative epithelial Znf217 expression in the $CD24^{Med}CD49f^{High}$ vs. $CD24^{High}CD49f^{Low}$ populations. Similar results were seen with the reference GAPDH. (E) Relative expression of Znf217 expression by rt-qPCR in primary mouse mammary epithelial cells following lentiviral infection with either pEiT vector or Znf217-pEiT in three separate samples. Each sample was tested by qPCR in triplicate relative to the reference TBP. These samples were used for microarray analysis. Graph shows the mean ± S.E.M. (F) Quantification and (G) brightfield images of mammosphere assay of Vo-PyMT cells overexpressing vector or Znf217. (H) Heat map of selected genes from gene expression microarray analysis enriched in primary MECs overexpressing Znf217. (I) Relative expression of Znf217 expression by rt-qPCR in primary mouse mammary epithelial cells following

lentiviral infection with either pEiT vector or Znf217-pEiT in three separate samples. Each sample was tested by qPCR in triplicate relative to the reference TBP. These samples were used for microarray analysis. Graph shows the mean ±S.E.M. (J) Rt-qPCR to validate microarray targets using the same samples used in (H) using HPRT as a reference in qPCR reactions. Similar results were obtained with GAPDH used as a reference (data not shown).

Figure 4. Znf217 overexpression in vivo increases rate of tumor progression, tumor heterogeneity and differentiation state. (A) Relative expression of Znf217 and EMT genes by RT-qPCR in the Vo-PyMT cell line overexpressing either vector or Znf217. Assay used the reference GAPDH. Similar results were seen using HPRT or TBP references. The cells used in this experiment had previously been sorted for fluorescent marker expression and were used for the Vo-PyMT transplants throughout this study. (B) Mammosphere assay of primary MECs infected with vector or Znf217-overexpressing lentivirus. (C) Quantification of mammosphere formation in primary MECs expressing vector or Znf217 after one week. Graph shows mean ± S.E.M., and samples were compared by unpaired t test. (D) Tumor-free survival over time in Vo-PyMT transplants (*P*=0.01; Logrank). (E) Tumor volume over time in Vo-PyMT transplants of Znf217 (n=8) versus vector (n=10) (*P*=0.007; ANOVA, repeated measures). (F) Final tumor weight in Vo-PyMT transplants (*P*=0.02; Mann-Whitney). Line represents median of vector (n=9) versus Znf217 (n=8). (G) H&E staining of MMTV-PyMT (PyMT MEC) tumors from transplants overexpressing vector (left) or Znf217 (center, right panels). Inserts are enlarged images of boxed regions and demonstrate heterogeneous pathology. (H) Immunofluorescence staining with anti-Keratin-8 (green), anti-alpha-smooth muscle actin (red)(arrows), and DNA (Hoechst; blue) in tumors derived from PyMT MEC transplants. (I) Immunofluorescence staining with anti-Keratin-8 (green), Keratin-14 (red), and DNA (blue) from PyMT MEC transplants. Arrows mark cells double positive for K8 and K14. (J) Quantification of progenitor cell population: K8+K14+ (*P*=0.002), % K8+K14+

(*P*=0.0002)(unpaired t tests). Bar graphs show mean ± S.E.M. HPF= 3 high-powered fields.

Figure 5. Znf217 overexpression in vivo increases lung metastasis. (A) Immunofluorescence with anti-E-cadherin (green) and DNA (blue) from Vo-PyMT transplants. Arrows mark regions with low E-cadherin expression. (B) Number of lung metastases per three (a) or five (b) high powered fields from (a) PyMT MEC (*P*=0.008) or (b) Vo-PyMT transplants (*P*=0.01; Mann-Whitney) with vector or Znf217 overexpression. Bar graph shows the mean ± S.E.M. (C) Metastatic burden from PyMT and Vo-PyMT transplants. Number of lung metastases per three (PyMT) or five (Vo-PyMT) high-powered fields divided by tumor weight from (a) PyMT MEC (*P*=0.003; Mann-Whitney) or (b) Vo-PyMT (*P*=0.32; Mann-Whitney) transplants with vector or Znf217 overexpression. Bar graph shows the mean ± S.E.M. Similar results were obtained using final tumor volume (data not shown). (D) H&E staining of lung metastases from PyMT MEC transplants. Arrows mark examples of metastases. (E) Metastasis-free survival based on high (n=41) vs. low (n=41) ZNF217 expression (*P*=0.01; Logrank) from (10).

Figure 6. Identification of triciribine as a candidate inhibitor of ZNF217-induced growth. (A) Response to neoadjuvant chemotherapy in breast cancer patients with high vs. low ZNF217 expression in tumors (a) from (16). Patients had a responsive (n=27) or nonresponsive (stable/progressive) disease (n=28) in response to treatment (*P*=0.01; Mann-Whitney). Lines mark the means. (b) from (25) (*P*<0.001; Mann-Whitney). Tumor samples were collected prior to treatment. Patients were responsive (pathological complete response; n=34) or nonresponsive (residual disease; n=34). Lines mark the means. (B) MCF7 cells were transiently transfected with scrambled or ZNF217 siRNA. 48h after transfection, cells were serum starved overnight and then treated 15 minute with heregulin as indicated. Lysates were collected at 72 hours post-transfection and blotted for the indicated proteins. (C) ZR75 cells were transiently transfected with scrambled or ZNF217 siRNA and processed as in (B). (D) PI3K and AKT

inhibitors do not promote ZNF217-dependent cell death. FACS analysis of cell death by Annexin V staining in MCF7 cells ±shRNA-ZNF217 or scramble control and treated for two days with control, 2 μM GDC0941, or 10 μM MK2206. (E) Treatment of MCF7 cells ± ZNF217-shRNA with bisacodyl in triplicate at the indicated concentrations (*P*=0.001; ANOVA). Similar results were obtained in at least three experiments. (F) Treatment of MCF7 cells ± ZNF217-shRNA with 10 μM triciribine at the indicated concentrations (*P*=0.001; ANOVA). Similar results were obtained with a second shRNA and in at least three experiments. (G) ZNF217 expression levels and (H) related triciribine GI50 concentrations in NCI60 panel breast cancer cell lines. Inset: Chemical structure of triciribine. (I) ZNF217 expression levels across triciribine GI50s in 30 breast cancer cell lines (15 each of cell lines expressing highest/lowest ZNF217)(r=-0.39; *P*=0.035; Spearman correlation). Two outliers are circled and identified by cell type and relevant mutations.

Figure 7. Triciribine inhibits Znf217 in vivo and in human cells. (A) Tumor burden growth rate of Vo-PyMT transplants treated with DMSO (solid lines) solution or triciribine (dotted line) (*P*<0.0001 based on genotype; *P*=0.02, genotype over time; ANOVA). Vo-PyMT transplants overexpressed vector (blue) or Znf217 (orange). Shown are the mean ± S.E.M. (B) Phospho-AKT (left) and phospho-MAPK (right) protein expression by immunohistochemistry in tissues from Vo-PyMT transplants that were treated with either control or triciribine. (C) MCF7 cells ± triciribine (also used in Figure 2D-F) were serum starved overnight and stimulated with heregulin/neuregulin-1ß for the indicated times. Cell lysates were blotted for the indicated proteins. (D) Human MCF-7-M1 subcutaneous xenografts treated with control or triciribine (50 mg/kg) at the indicated time post-transplant. Ticks show mean tumor burden ± standard deviation. (E) Model of pathways downstream from Znf217. Znf217 overexpression promotes phospho-AKT and phospho-MAPK. This activation is associated with increased tumor burden, chemotherapy resistance, and mammosphere formation. Triciribine can block these phenotypes of Znf217 overexpression. (F) Triciribine induces

synthetic lethality with doxorubicin in culture. Stable HBL100 MECs (low ZNF217, low adenosine kinase expression) (± ZNF217) were treated with triciribine and doxorubicin at the indicated concentrations and monitored for cell death using Annexin V staining (P=0.0002; ANOVA). All doxorubicin-treated samples were statistically different (P<0.05; Bonferroni posttest), whereas triciribine treatment alone did not promote statistically significant results. Graph shows mean ± S.E.M. (G) Model of Znf217 function. Increased Znf217 promotes increased ErbB3 expression and activation of downstream signaling events during tumor progression. ZNF217 may also activate other receptor tyrosine kinases (RTKs) that in turn lead to activation of AKT or MAPK pathways. In vivo during tumor progression, triciribine is able to block signaling events downstream of Znf217 overexpression.

References

1. Collins C, Rommens JM, Kowbel D, Godfrey T, Tanner M, Hwang SI, et al. Positional cloning of ZNF217 and NABC1: genes amplified at 20q13.2 and overexpressed in breast carcinoma. Proc Natl Acad Sci U S A. 1998;95:8703-8.
2. Collins C, Volik S, Kowbel D, Ginzinger D, Ylstra B, Cloutier T, et al. Comprehensive genome sequence analysis of a breast cancer amplicon. Genome Res. 2001;11:1034-42.
3. You A, Tong JK, Grozinger CM, Schreiber SL. CoREST is an integral component of the CoREST- human histone deacetylase complex. Proc Natl Acad Sci U S A. 2001;98:1454-8.
4. Shi Y, Sawada J, Sui G, Affar el B, Whetstine JR, Lan F, et al. Coordinated histone modifications mediated by a CtBP co-repressor complex. Nature. 2003;422:735-8.
5. Quinlan KG, Nardini M, Verger A, Francescato P, Yaswen P, Corda D, et al. Specific recognition of ZNF217 and other zinc finger proteins at a surface groove of C-terminal binding proteins. Mol Cell Biol. 2006;26:8159-72.
6. Cowger JJ, Zhao Q, Isovic M, Torchia J. Biochemical characterization of the zinc-finger protein 217 transcriptional repressor complex: identification of a ZNF217 consensus recognition sequence. Oncogene. 2007;26:3378-86.
7. Thillainadesan G, Isovic M, Loney E, Andrews J, Tini M, Torchia J. Genome analysis identifies the p15ink4b tumor suppressor as a direct target of the ZNF217/CoREST complex. Mol Cell Biol. 2008;28:6066-77.
8. Banck MS, Li S, Nishio H, Wang C, Beutler AS, Walsh MJ. The ZNF217 oncogene is a candidate organizer of repressive histone modifiers. Epigenetics. 2009;4:100-6.
9. Nonet GH, Stampfer MR, Chin K, Gray JW, Collins CC, Yaswen P. The ZNF217 gene amplified in breast cancers promotes immortalization of human mammary epithelial cells. Cancer Res. 2001;61:1250-4.
10. Krig SR, Jin VX, Bieda MC, O'Geen H, Yaswen P, Green R, et al. Identification of genes directly regulated by the oncogene ZNF217 using chromatin immunoprecipitation (ChIP)-chip assays. J Biol Chem. 2007;282:9703-12.
11. Blick T, Hugo H, Widodo E, Waltham M, Pinto C, Mani SA, et al. Epithelial mesenchymal transition traits in human breast cancer cell lines parallel the CD44(hi/)CD24 (lo/-) stem cell phenotype in human breast cancer. Journal of mammary gland biology and neoplasia. 2010;15:235-52.
12. Polyak K, Weinberg RA. Transitions between epithelial and mesenchymal states: acquisition of malignant and stem cell traits. Nat Rev Cancer. 2009;9:265-73.
13. Thiery JP, Acloque H, Huang RY, Nieto MA. Epithelial-mesenchymal transitions in development and disease. Cell. 2009;139:871-90.

14. Mani SA, Guo W, Liao MJ, Eaton EN, Ayyanan A, Zhou AY, et al. The epithelial-mesenchymal transition generates cells with properties of stem cells. Cell. 2008;133:704-15.
15. Chin K, DeVries S, Fridlyand J, Spellman PT, Roydasgupta R, Kuo WL, et al. Genomic and transcriptional aberrations linked to breast cancer pathophysiologies. Cancer Cell. 2006;10:529-41.
16. Sorlie T, Perou CM, Fan C, Geisler S, Aas T, Nobel A, et al. Gene expression profiles do not consistently predict the clinical treatment response in locally advanced breast cancer. Molecular cancer therapeutics. 2006;5:2914-8.
17. Wong DJ, Liu H, Ridky TW, Cassarino D, Segal E, Chang HY. Module map of stem cell genes guides creation of epithelial cancer stem cells. Cell stem cell. 2008;2:333-44.
18. Woodward WA, Chen MS, Behbod F, Rosen JM. On mammary stem cells. Journal of cell science. 2005;118:3585-94.
19. Wang XY, Yin Y, Yuan H, Sakamaki T, Okano H, Glazer RI. Musashi1 modulates mammary progenitor cell expansion through proliferin-mediated activation of the Wnt and Notch pathways. Mol Cell Biol. 2008;28:3589-99.
20. Villadsen R, Fridriksdottir AJ, Ronnov-Jessen L, Gudjonsson T, Rank F, LaBarge MA, et al. Evidence for a stem cell hierarchy in the adult human breast. J Cell Biol. 2007;177:87-101.
21. McCaffrey LM, Macara IG. The Par3/aPKC interaction is essential for end bud remodeling and progenitor differentiation during mammary gland morphogenesis. Genes Dev. 2009;23:1450-60.
22. Gudjonsson T, Villadsen R, Nielsen HL, Ronnov-Jessen L, Bissell MJ, Petersen OW. Isolation, immortalization, and characterization of a human breast epithelial cell line with stem cell properties. Genes Dev. 2002;16:693-706.
23. Minn AJ, Gupta GP, Siegel PM, Bos PD, Shu W, Giri DD, et al. Genes that mediate breast cancer metastasis to lung. Nature. 2005;436:518-24.
24. Li X, Lewis MT, Huang J, Gutierrez C, Osborne CK, Wu MF, et al. Intrinsic resistance of tumorigenic breast cancer cells to chemotherapy. Journal of the National Cancer Institute. 2008;100:672-9.
25. Hess KR, Anderson K, Symmans WF, Valero V, Ibrahim N, Mejia JA, et al. Pharmacogenomic predictor of sensitivity to preoperative chemotherapy with paclitaxel and fluorouracil, doxorubicin, and cyclophosphamide in breast cancer. J Clin Oncol. 2006;24:4236-44.
26. Krig SR, Miller JK, Frietze S, Beckett LA, Neve RM, Farnham PJ, et al. ZNF217, a candidate breast cancer oncogene amplified at 20q13, regulates expression of the ErbB3 receptor tyrosine kinase in breast cancer cells. Oncogene. 2010;29:5500-10.
27. Huang G, Krig S, Kowbel D, Xu H, Hyun B, Volik S, et al. ZNF217 suppresses cell death associated with chemotherapy and telomere dysfunction. Hum Mol Genet. 2005;14:3219-25.
28. Schilcher RB, Haas CD, Samson MK, Young JD, Baker LH. Phase I evaluation and clinical pharmacology of tricyclic nucleoside 5'-phosphate using a weekly intravenous regimen. Cancer Res. 1986;46:3147-51.

29. Feun LG, Savaraj N, Bodey GP, Lu K, Yap BS, Ajani JA, et al. Phase I study of tricyclic nucleoside phosphate using a five-day continuous infusion schedule. Cancer research. 1984;44:3608-12.
30. Garrett CR, Coppola D, Wenham RM, Cubitt CL, Neuger AM, Frost TJ, et al. Phase I pharmacokinetic and pharmacodynamic study of triciribine phosphate monohydrate, a small-molecule inhibitor of AKT phosphorylation, in adult subjects with solid tumors containing activated AKT. Invest New Drugs. 2011;29:1381-9.
31. Hoffman K, Holmes FA, Fraschini G, Esparza L, Frye D, Raber MN, et al. Phase I-II study: triciribine (tricyclic nucleoside phosphate) for metastatic breast cancer. Cancer Chemother Pharmacol. 1996;37:254-8.
32. Neve RM, Chin K, Fridlyand J, Yeh J, Baehner FL, Fevr T, et al. A collection of breast cancer cell lines for the study of functionally distinct cancer subtypes. Cancer Cell. 2006;10:515-27.
33. Lu CH, Wyszomierski SL, Tseng LM, Sun MH, Lan KH, Neal CL, et al. Preclinical testing of clinically applicable strategies for overcoming trastuzumab resistance caused by PTEN deficiency. Clin Cancer Res. 2007;13:5883-8.
34. Balasis ME, Forinash KD, Chen YA, Fulp WJ, Coppola D, Hamilton AD, et al. Combination of farnesyltransferase and Akt inhibitors is synergistic in breast cancer cells and causes significant breast tumor regression in ErbB2 transgenic mice. Clinical cancer research : an official journal of the American Association for Cancer Research. 2011;17:2852-62.
35. Yang L, Dan HC, Sun M, Liu Q, Sun XM, Feldman RI, et al. Akt/protein kinase B signaling inhibitor-2, a selective small molecule inhibitor of Akt signaling with antitumor activity in cancer cells overexpressing Akt. Cancer Res. 2004;64:4394-9.
36. Berndt N, Yang H, Trinczek B, Betzi S, Zhang Z, Wu B, et al. The Akt activation inhibitor TCN-P inhibits Akt phosphorylation by binding to the PH domain of Akt and blocking its recruitment to the plasma membrane. Cell Death Differ. 2010;17:1795-804.
37. She QB, Halilovic E, Ye Q, Zhen W, Shirasawa S, Sasazuki T, et al. 4E-BP1 is a key effector of the oncogenic activation of the AKT and ERK signaling pathways that integrates their function in tumors. Cancer Cell. 2010;18:39-51.
38. Hoeflich KP, O'Brien C, Boyd Z, Cavet G, Guerrero S, Jung K, et al. In vivo antitumor activity of MEK and phosphatidylinositol 3-kinase inhibitors in basal-like breast cancer models. Clin Cancer Res. 2009;15:4649-64.
39. Hollestelle A, Nagel JH, Smid M, Lam S, Elstrodt F, Wasielewski M, et al. Distinct gene mutation profiles among luminal-type and basal-type breast cancer cell lines. Breast cancer research and treatment. 2010;121:53-64.
40. She QB, Chandarlapaty S, Ye Q, Lobo J, Haskell KM, Leander KR, et al. Breast tumor cells with PI3K mutation or HER2 amplification are selectively addicted to Akt signaling. PLoS One. 2008;3:e3065.
41. Li P, Maines-Bandiera S, Kuo WL, Guan Y, Sun Y, Hills M, et al. Multiple roles of the candidate oncogene ZNF217 in ovarian epithelial neoplastic progression. Int J Cancer. 2007;120:1863-73.

42. Buttitta L, Tanaka TS, Chen AE, Ko MS, Fan CM. Microarray analysis of somitogenesis reveals novel targets of different WNT signaling pathways in the somitic mesoderm. Developmental biology. 2003;258:91-104.
43. Li Y, Welm B, Podsypanina K, Huang S, Chamorro M, Zhang X, et al. Evidence that transgenes encoding components of the Wnt signaling pathway preferentially induce mammary cancers from progenitor cells. Proc Natl Acad Sci U S A. 2003;100:15853-8.
44. Korkaya H, Paulson A, Charafe-Jauffret E, Ginestier C, Brown M, Dutcher J, et al. Regulation of mammary stem/progenitor cells by PTEN/Akt/beta-catenin signaling. PLoS Biol. 2009;7:e1000121.
45. Du Z, Podsypanina K, Huang S, McGrath A, Toneff MJ, Bogoslovskaia E, et al. Introduction of oncogenes into mammary glands in vivo with an avian retroviral vector initiates and promotes carcinogenesis in mouse models. Proc Natl Acad Sci U S A. 2006;103:17396-401.

A Overall survival

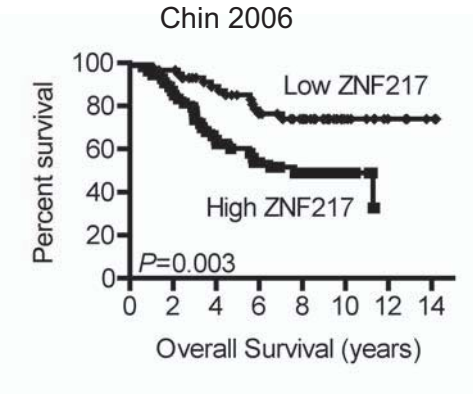

B Relapse-Free Survival

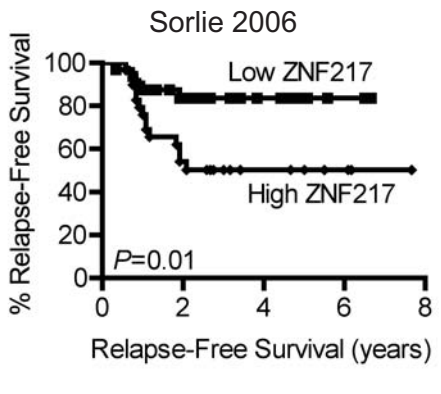

C ER+ Her2- LN- patients

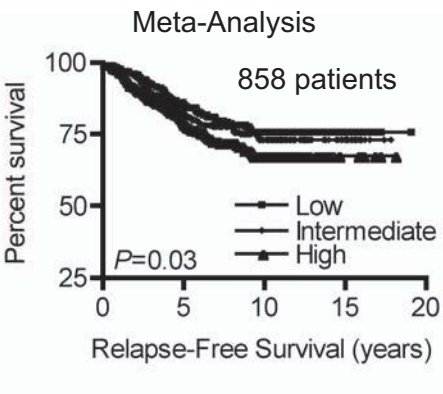

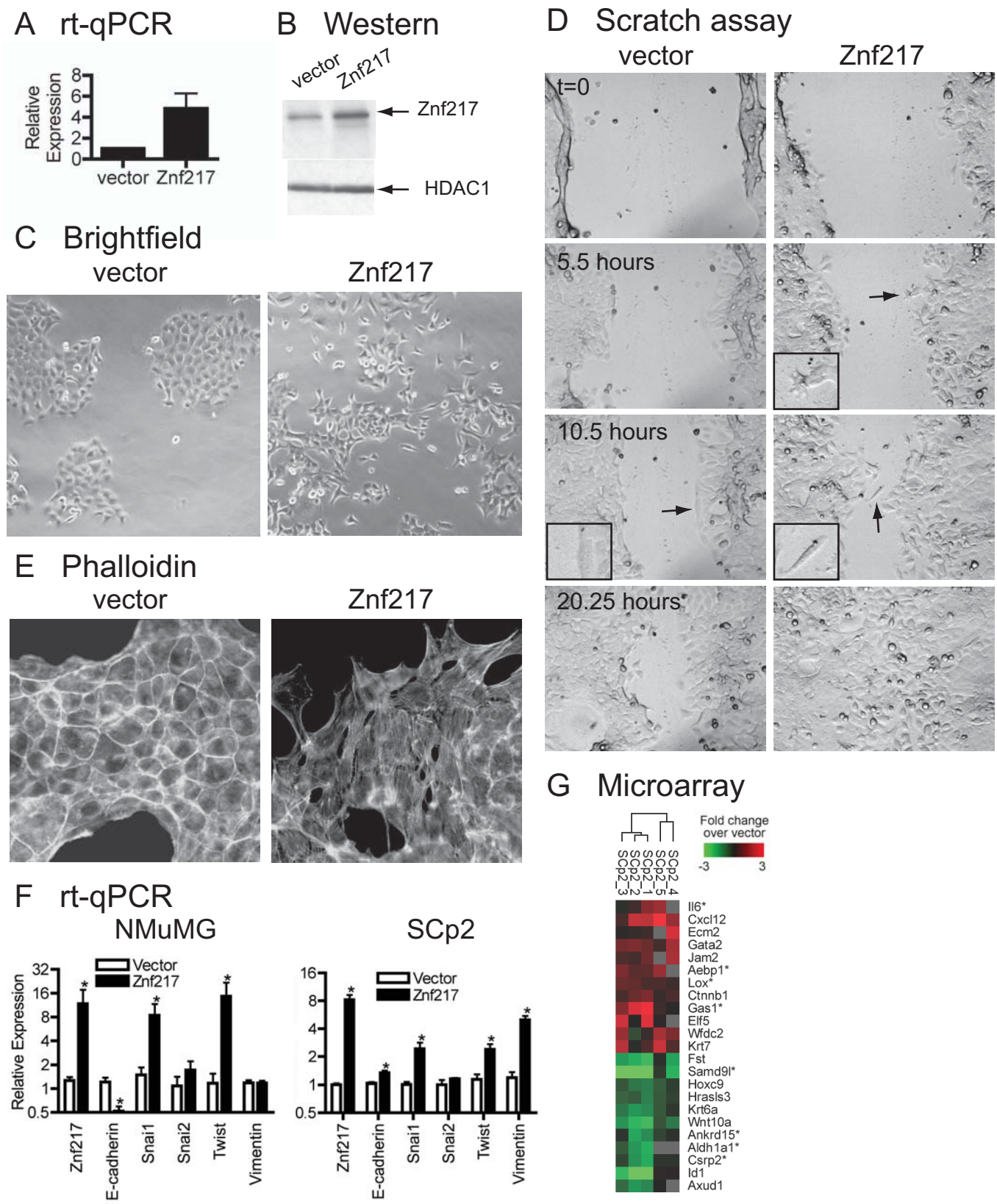
A rt-qPCR
Relative Expression
vector Znf217
B Western
vector
Znf217
Znf217
HDAC1
C Brightfield
vector
Znf217
D Scratch assay
vector
Znf217
t=0
5.5 hours
10.5 hours
20.25 hours
E Phalloidin
vector
Znf217
F rt-qPCR
NMuMG
SCp2
Vector
Znf217
Relative Expression
Znf217
E-cadherin
Snai1
Snai2
Twist
Vimentin
G Microarray
Fold change over vector
-3
3
Il6*
Cxcl12
Ecm2
Gata2
Jam2
Aebp1*
Lox*
Ctnnb1
Gas1*
Elf5
Wfdc2
Krt7
Fst
Samd9l*
Hoxc9
Hrasls3
Krt6a
Wnt10a
Ankrd15*
Aldh1a1*
Csrp2*
Id1
Axud1

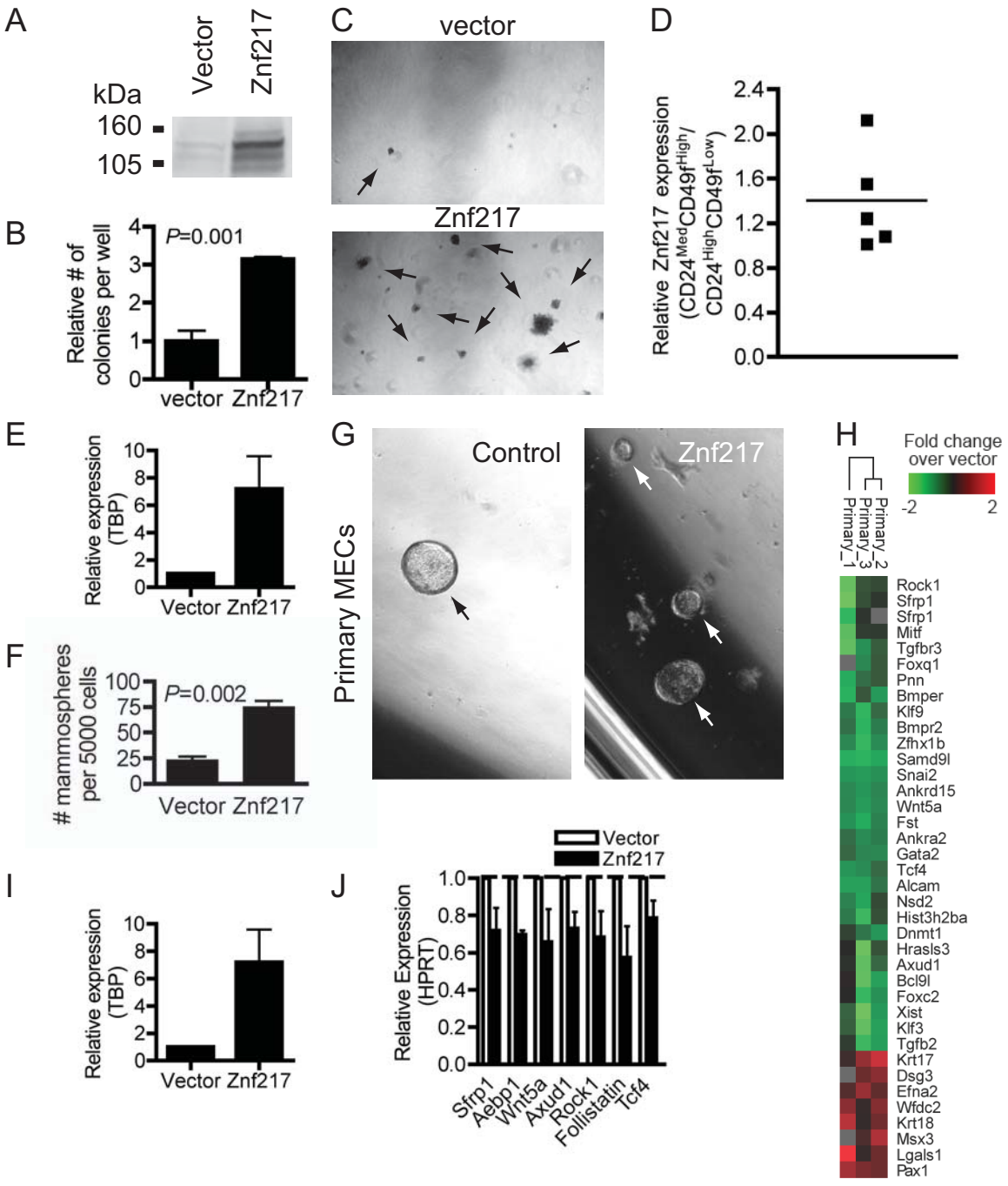
A
Vector
Znf217
kDa
160
105
B
Relative # of colonies per well
P=0.001
vector Znf217
C
vector
Znf217
D
Relative Znf217 expression (CD24MedCD49fHigh/ CD24HighCD49fLow)
E
Relative expression (TBP)
Vector Znf217
F
# mammospheres per 5000 cells
P=0.002
Vector Znf217
G
Primary MECs
Control
Znf217
H
Fold change over vector
-2
2
Primary_1
Primary_3
Primary_2
Rock1
Sfrp1
Sfrp1
Mitf
Tgfbr3
Foxq1
Pnn
Bmper
Klf9
Bmpr2
Zfhx1b
Samd9l
Snai2
Ankrd15
Wnt5a
Fst
Ankra2
Gata2
Tcf4
Alcam
Nsd2
Hist3h2ba
Dnmt1
Hrasls3
Axud1
Bcl9l
Foxc2
Xist
Klf3
Tgfb2
Krt17
Dsg3
Efna2
Wfdc2
Krt18
Msx3
Lgals1
Pax1
I
Relative expression (TBP)
Vector Znf217
J
Vector
Znf217
Relative Expression (HPRT)
Sfrp1
Aebp1
Wnt5a
Axud1
Rock1
Follistatin
Tcf4

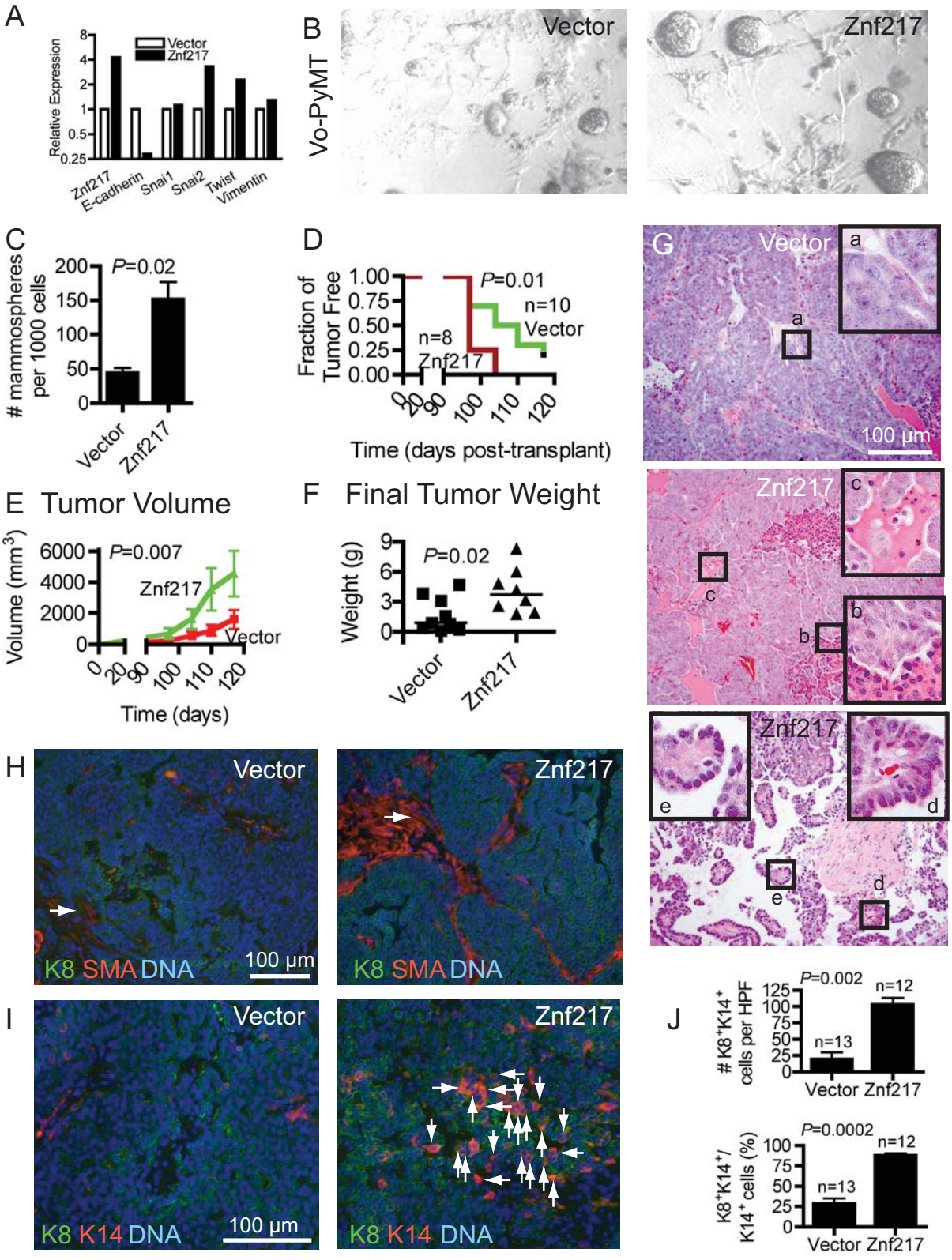
A
Relative Expression
Vector
Znf217
Znf217
E-cadherin
Snai1
Snai2
Twist
Vimentin
B
Vo-PyMT
Vector
Znf217
C
# mammospheres per 1000 cells
P=0.02
Vector
Znf217
D
Fraction of Tumor Free
P=0.01
n=10
Vector
n=8
Znf217
Time (days post-transplant)
E Tumor Volume
Volume (mm3)
P=0.007
Znf217
Vector
Time (days)
F Final Tumor Weight
Weight (g)
P=0.02
Vector
Znf217
G
Vector
Znf217
Znf217
100 µm
H
Vector
Znf217
K8 SMA DNA
100 µm
I
Vector
Znf217
K8 K14 DNA
100 µm
J
# K8+K14+ cells per HPF
P=0.002
n=13
n=12
Vector Znf217
K8+K14+/ K14+ cells (%)
P=0.0002
n=13
n=12
Vector Znf217

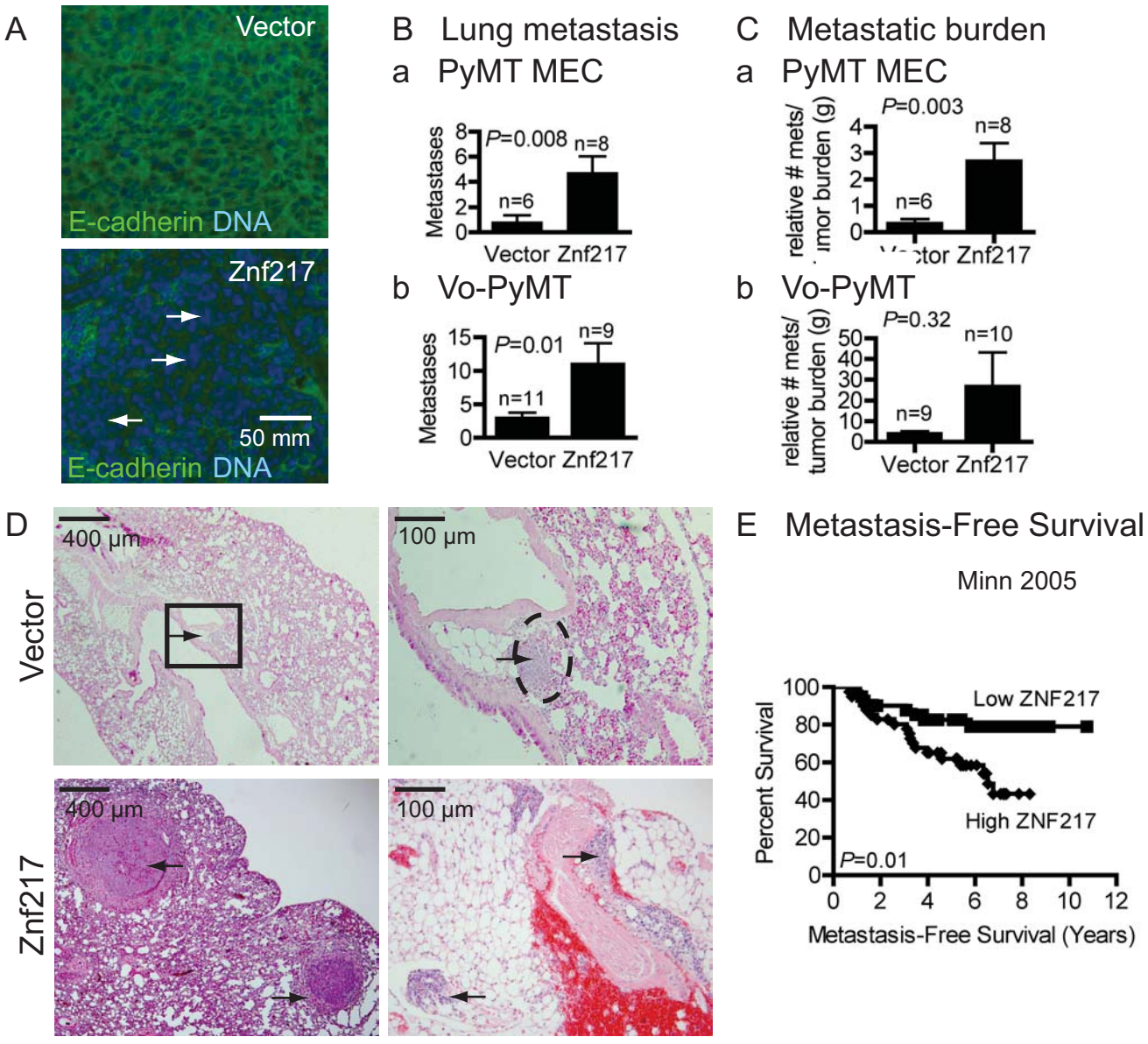
A
Vector
E-cadherin DNA
Znf217
50 mm
E-cadherin DNA
B Lung metastasis
a PyMT MEC
Metastases
P=0.008
n=8
n=6
Vector Znf217
b Vo-PyMT
Metastases
P=0.01
n=9
n=11
Vector Znf217
C Metastatic burden
a PyMT MEC
relative # mets/ tumor burden (g)
P=0.003
n=8
n=6
Vector Znf217
b Vo-PyMT
relative # mets/ tumor burden (g)
P=0.32
n=10
n=9
Vector Znf217
D
Vector
Znf217
400 µm
100 µm
400 µm
100 µm
E Metastasis-Free Survival
Minn 2005
Percent Survival
Low ZNF217
High ZNF217
P=0.01
Metastasis-Free Survival (Years)

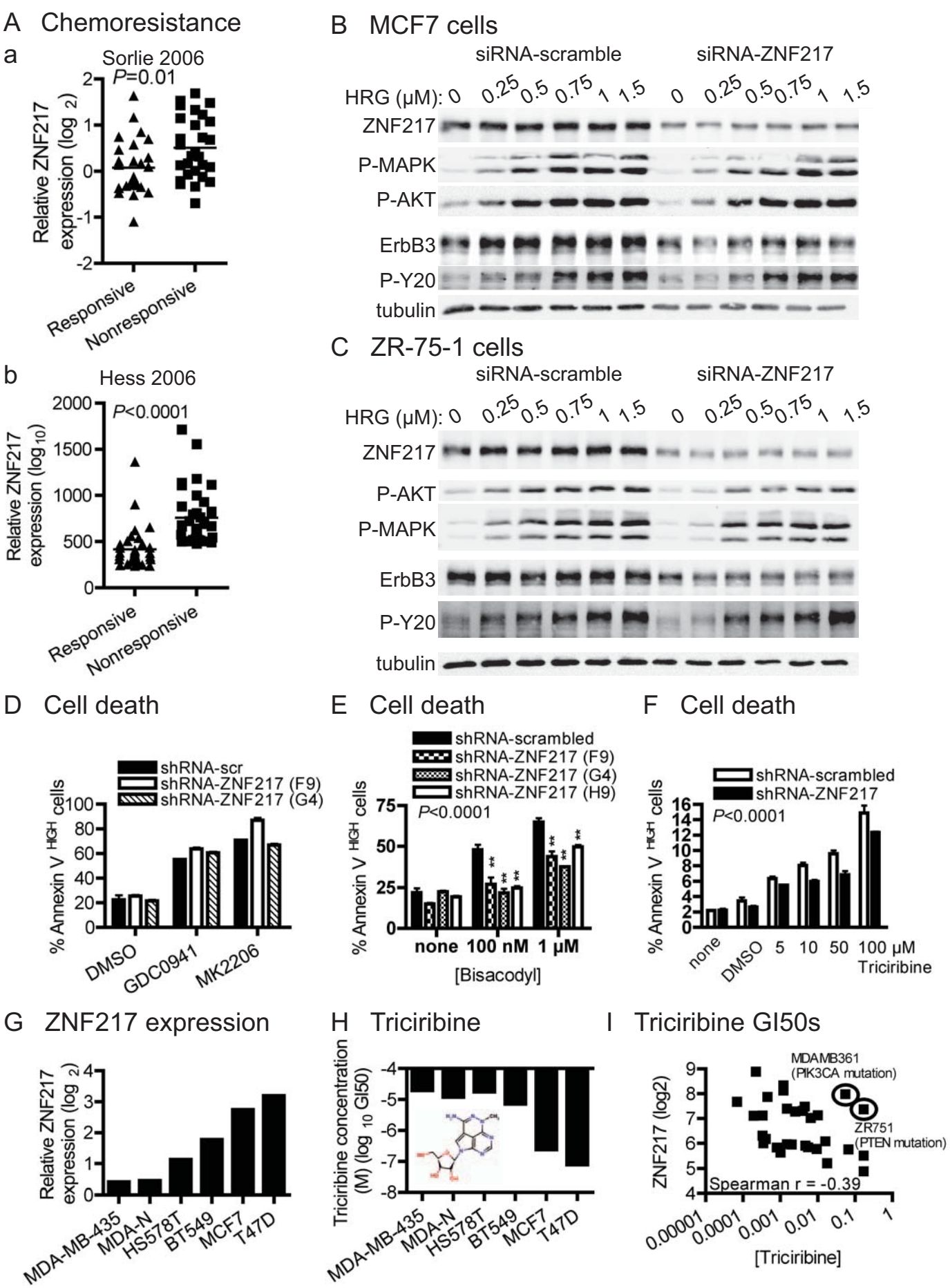
A Chemoresistance
a
Sorlie 2006
P=0.01
Relative ZNF217 expression (log 2)
Responsive
Nonresponsive
b
Hess 2006
P<0.0001
Relative ZNF217 expression (log 10)
Responsive
Nonresponsive
B MCF7 cells
siRNA-scramble
siRNA-ZNF217
HRG (μM): 0 0.25 0.5 0.75 1 1.5 0 0.25 0.5 0.75 1 1.5
ZNF217
P-MAPK
P-AKT
ErbB3
P-Y20
tubulin
C ZR-75-1 cells
siRNA-scramble
siRNA-ZNF217
HRG (μM): 0 0.25 0.5 0.75 1 1.5 0 0.25 0.5 0.75 1 1.5
ZNF217
P-AKT
P-MAPK
ErbB3
P-Y20
tubulin
D Cell death
shRNA-scr
shRNA-ZNF217 (F9)
shRNA-ZNF217 (G4)
% Annexin V HIGH cells
DMSO
GDC0941
MK2206
E Cell death
shRNA-scrambled
shRNA-ZNF217 (F9)
shRNA-ZNF217 (G4)
shRNA-ZNF217 (H9)
P<0.0001
% Annexin V HIGH cells
none 100 nM 1 μM
[Bisacodyl]
F Cell death
shRNA-scrambled
shRNA-ZNF217
P<0.0001
% Annexin V HIGH cells
none DMSO 5 10 50 100 μM
Triciribine
G ZNF217 expression
Relative ZNF217 expression (log 2)
MDA-MB-435
MDA-N
HS578T
BT549
MCF7
T47D
H Triciribine
Triciribine concentration (M) (log 10 GI50)
MDA-MB-435
MDA-N
HS578T
BT549
MCF7
T47D
I Triciribine GI50s
MDAMB361
(PIK3CA mutation)
ZR751
(PTEN mutation)
ZNF217 (log2)
Spearman r = -0.39
[Triciribine]

A Tumor Burden

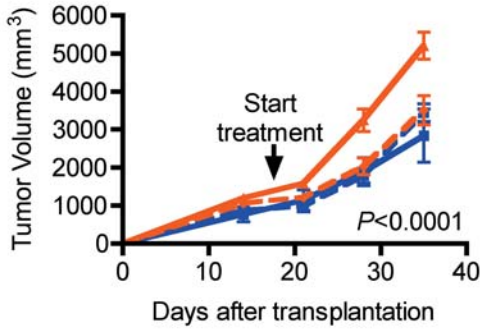

B Phospho-AKT Phospho-MAPK

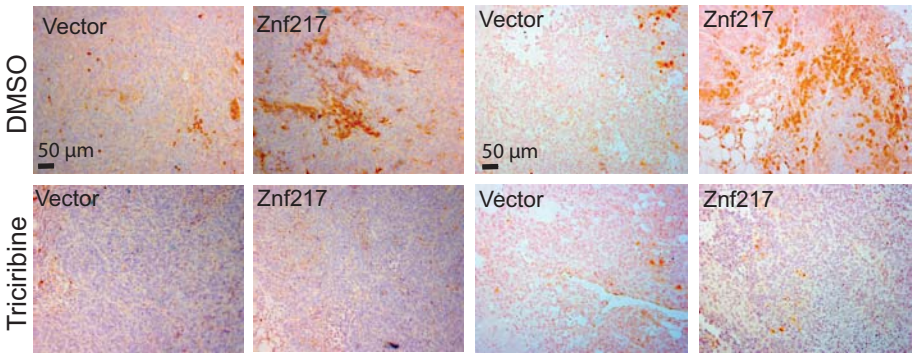

C Triciribine + HRG

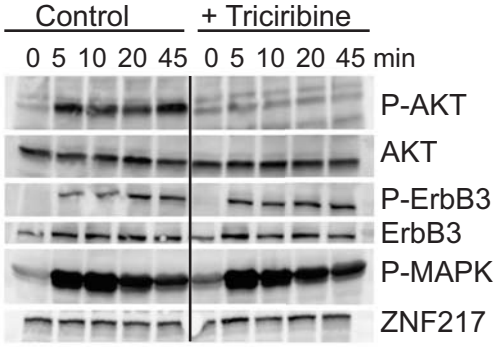

D MCF-7 xenografts

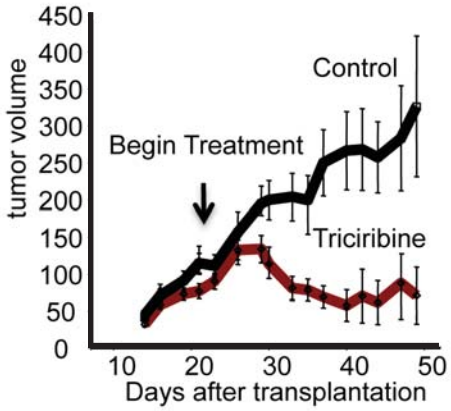

E

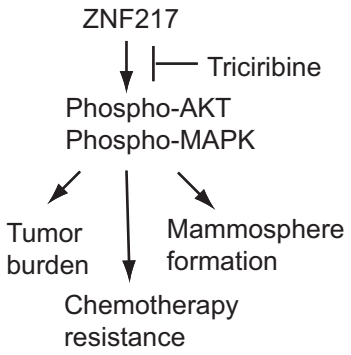

F Triciribine and Doxorubicin

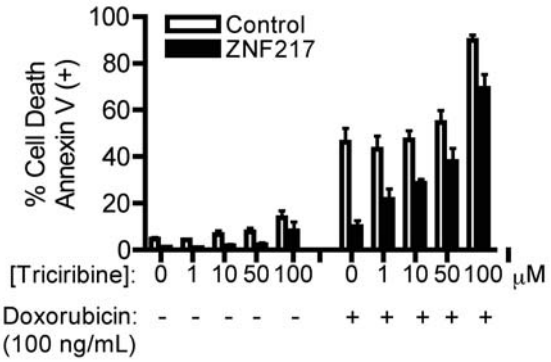

G